LAWRENCE
LIVERMORE
NATIONAL
LABORATORY

LLNL-PROC-403194

PBXN-9 Ignition Kinetics and Deflagration Rates

E.A. Glascoe, J.L. Maienschein, A.K. Burnham,
J.G. Koerner, P.C. Hsu, A.P. Wemhoff

April 25, 2008

55th JANNAF Propulsion Meeting
Newton, MA, United States
May 12, 2008 through May 16, 2008

Disclaimer

This work performed under the auspices of the U. S. Department of Energy by Lawrence Livermore National Laboratory under Contract DE-AC52-07NA27344.

PBXN-9 IGNITION KINETICS AND DEFLAGRATION RATES

E.A. Glascoe, J.L. Maienschein, A.K. Burnham, J.G. Koerner, P.C. Hsu, A.P. Wemhoff
Lawrence Livermore National Laboratory Energetic Materials Center
Livermore, CA

ABSTRACT

The ignition kinetics and deflagration rates of PBXN-9 were measured using specially designed instruments at LLNL and compared with previous work on similar HMX based materials. Ignition kinetics were measured based on the One Dimensional Time-to-Explosion combined with ALE3D modeling. Results of these experiments indicate that PBXN-9 behaves much like other HMX based materials (i.e. LX-04, LX-07, LX-10 and PBX-9501) and the dominant factor in these experiments is the type of explosive, not the type of binder/plasticizer. In contrast, the deflagration behavior of PBXN-9 is quite different from similar high weight percent HMX based materials (i.e LX-10, LX-07 and PBX-9501). PBXN-9 burns in a laminar manner over the full pressure range studied (0-310 MPa) unlike LX-10, LX-07, and PBX-9501. The difference in deflagration behavior is attributed to the nature of the binder/plasticizer alone or in conjunction with the volume of binder present in PBXN-9.

INTRODUCTION

A thorough understanding of the response of energetic materials to thermal stimulus is of broad interest to the explosives and propellants communities. The development of safe handling and storage methods and establishment of optimal use conditions requires prior knowledge of thermal response of the material under ambient and elevated pressures and temperatures. In addition, thermal decomposition kinetics are an established method for exploring the underlying fundamental physics and chemistry of a materials.

Both thermal and mechanical stimuli can initiate a reaction in an energetic material. The initial steps are typically endothermic; however, the material rapidly switches over to exothermic reactions capable of accelerating the decomposition or combustion. In insulated and/or contained environments, the pressure and temperature can rise quickly as the material reacts resulting in an acceleration of the reaction until runaway conditions are reached. Accurate knowledge of the reaction rates at conditions typical of those in accelerating reactions is necessary to understand and predict the violence of the ensuing explosion. Hydrodynamic calculations indicate that reacting materials can achieve pressures in the hundreds of MPa range (several kbar) and higher. Therefore, measurements of the laminar deflagration rate and thermal ignition kinetics at high pressures and temperatures are needed for accurate prediction of reaction violence through computer simulations.[1,2]

Using custom designed instruments and ALE3D modeling we have explored the thermal response of the energetic material PBXN-9 (92 wt% HMX, 6 wt% dioctyl adipate (DOA), 2 wt% carboxyl-terminated polybutadiene (HYTEMP 4544)). Deflagration rates were measured as a function of pressure from 0 – 310 MPa using the LLNL high pressure strand burner. One dimensional time to explosion (ODTX) measurements were made between 161 and 227 ^{o}C and ALE3D modeling was used to determine the kinetic parameters for thermal ignition. Comparison of the PBXN-9 results with energetic materials with a similar HMX content indicate that the binder/plasticizer combination in PBXN-9 play a key role in the thermal response of the material.[*]

EXPERIMENTS AND CALCULATIONS

LLNL HIGH PRESSURE STRAND BURNER

The LLNL High Pressure Strand Burner, shown schematically in Figure 1, combines the features of a traditional closed-bomb burner with those of a traditional strand burner. It contains a deflagrating sample in a small volume, high-pressure chamber. Simultaneous temporal pressure and burn front time-of-arrival measurements yield the laminar deflagration rate for a range of pressures and provide insight into deflagration uniformity in one experiment. Pressure is measured using a pressure transducer and a load cell, and burn front arrival is detected by the burning-through of thin silver wires embedded in the sample. High speed digital scopes capture the data for subsequent analysis.

The strand burner has an internal volume of approximately 75 cm^3 (4.6 in^3) and is designed to reach pressures of 1 GPa (150,000 psi). The pressure vessel body is built from two concentric shells with interference between them to put the inner shell in compression. The standard inner liner and the top and bottom closures are fabricated from hardened S-5 tool steel, which is high strength but also brittle and prone to corrosion. The S-5 tool steel is suitable for experiments with PBXN-9 which generates little or no corrosive gasses. The top end plug is equipped with gas inlet and outlet ports and a pressure transducer, while the bottom end plug holds a prewired base and high pressure feed-throughs for the burn wires, igniter wires, and thermocouples. The pressure transducer is a Kistler model 6213B. The load cell is Omega model LCTB-150K. The commercial sensor was calibrated to NIST standards by the manufacturer, and the load cell was calibrated against the Kistler transducer.

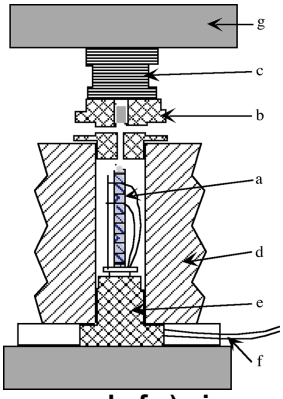

Figure 1. Strand burner schematic composed of a) nine segment burn sample with burn wires evenly spaced between segments (only two wires shown for clarity) and igniter on top, b) top plug with inlet and outlet ports and pressure transducer in center, c) load cell, d) pressure vessel, e) bottom plug with wire feed-throughs, f) signal wires to electronics, g) load frame (top and bottom).

The burn sample, shown in Figure 2, consists of nine 6.35-mm (0.25 in) length by 6.35-mm diameter cylinders stacked on end. Seventy-five-micron (3 mil) diameter silver burn wires are inserted radially in a groove between each pair of pellets. After assembly, the cylindrical surface of the sample is coated with epoxy to inhibit burning on that surface. This limits the flame front to the cross-sectional surface of the cylinder. An igniter train consisting of an igniter wire, approximately 110 mg of B/KNO_3, and a thin, 30 mg pressed HNS pellet ignites the burn sample on the top end of the cylinder. Further details are available in the literature.[3]

Figure 2. Sample holder and explosive sample. Burn wires are inserted through holes in Teflon® tube into sample. B/KNO_3 and HNS igniter and cardboard tube is on top, with igniter wires leading to it. Thermocouple in front is used to monitor temperature inside pressure vessel.

To conduct a measurement, the sample is mounted into a pre-wired base that carries the signal wires through high pressure feed-throughs in the bottom plug of the pressure vessel. The sample and bottom plug are then inserted into the pressure vessel. The system is pressurized to the desired starting pressure (up to 400 MPa or 60,000 psi) with argon and remotely sealed by immersing the inlet and outlet argon gas lines in liquid nitrogen. The argon freezes and acts as a remotely actuated pressure isolation valve with no moving parts or seals to maintain. Once the desired pressure is reached, sample deflagration is initiated, and temporal pressure and burn front time-of-arrival data are recorded. Following the run, the pressure is released by remotely removing the outlet argon gas line from the liquid nitrogen.

Typical pressure and flame front time-of-arrival data are shown in Figure 3. These results represent a well behaved burn because the wires are burned in order and the pressure rise stops after the last burn wire.

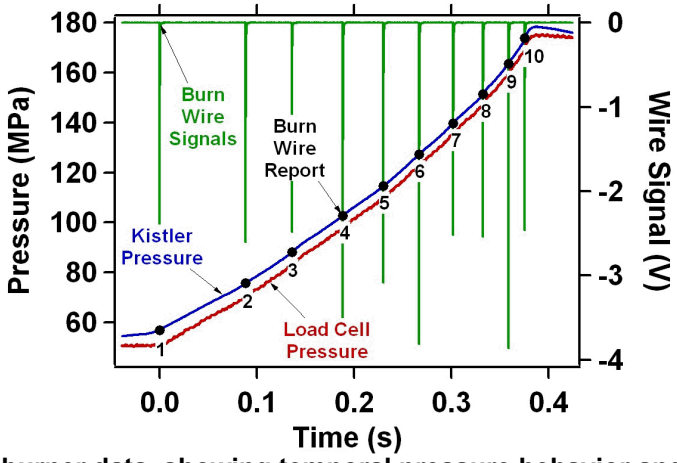

Figure 3. Typical strand burner data, showing temporal pressure behavior and flame-front time-of-arrival signals resulting from the burn wires.

The burn wire electronics provide a well defined signal, with measured rise times less than 40 microseconds. The wires burn through reproducibly, with wires mounted at the same location in the sample showing a standard deviation of 1-2 milliseconds. The wires do take several milliseconds to burn through; however, this time is essentially independent of initial pressure and temperature conditions and therefore does not affect the deflagration rate calculation by differences in time-of-arrival. The burn wire at the bottom of the stack does not burn through unless enough energetic material is placed below it to provide several milliseconds of burning once the flame front has passed. Burn wires are recorded in a way which allows for unambiguous assignment of each signal to a particular wire. This is necessary, as wires occasionally report out of sequence if broken by debris in the bomb chamber.

The burn wire data should cover the time span of the pressure signal. Any significant deviation from this indicates anomalous behavior. For example, the report of all burn wires before the pressure reaches a maximum indicates that the deflagration front passes rapidly down the sample and leaves still-reacting material behind. This behavior is indicative of flame spread through the sample or of propagation of the flame down the side of the sample; however, the epoxy coating should inhibit the latter.

To calculate deflagration rate as a function of pressure, the length and time-of-arrival for each pair of pellets is used, and the corresponding average pressure for this segment of the sample is calculated. The temporal pressure data can be used to calculate vivacity and surface area.[4-6]

LLNL One-Dimensional Time to Explosion (ODTX) Apparatus

ODTX experiments measure times to explosion and minimum ignition temperatures of high explosives. These measurements provide insight into the relative ease of thermal ignition and allow for the determination of kinetic parameters. The experiment involves isothermally heating a 12.7-m-diameter spherical sample in a 12.7-mm-diameter spherical cavity between two aluminum anvils. The apparatus is pictured in Figure 4 and key components are labeled.

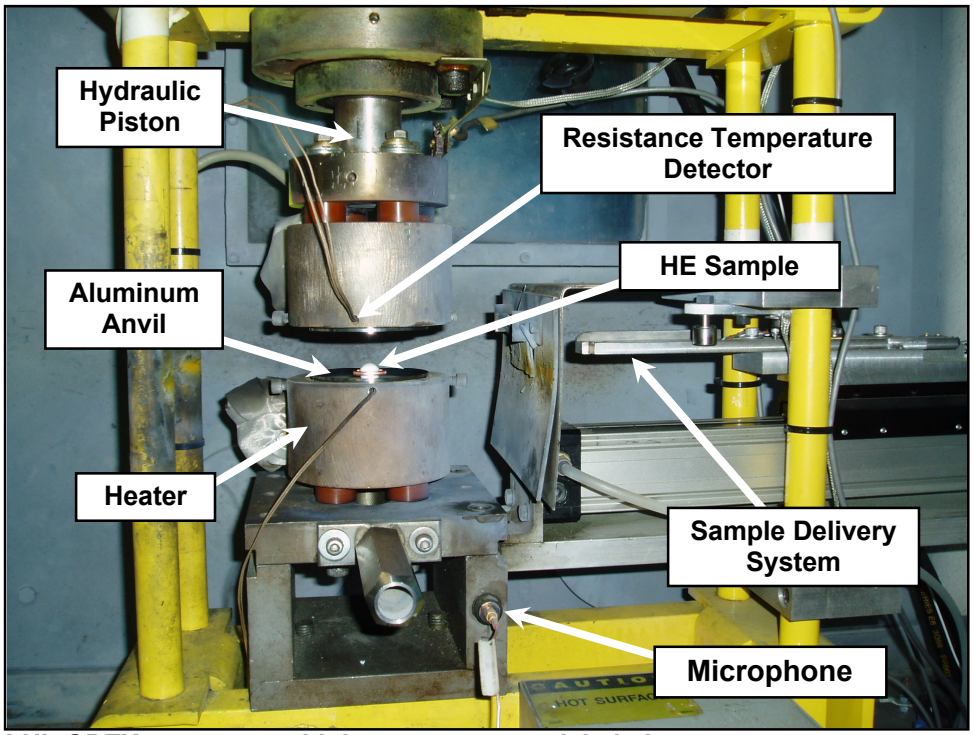

Figure 4. LLNL ODTX apparatus with key components labeled.

The sample is remotely delivered to the anvil cavity with the sample delivery system. A cross-sectional view of the anvil cavity is shown in Figure 5.

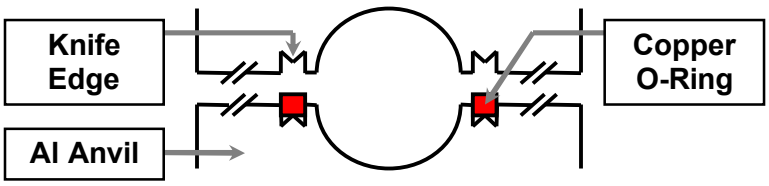

Figure 5. Cross-sectional view of 12.7-mm diameter spherical anvil cavity.

The hydraulic piston drives the top heater and anvil downward towards the bottom heater and anvil. A copper o-ring, if present, allows for the confinement pressure to reach approximately 150 MPa when compressed by the two knife-edges on the aluminum anvils. The top and bottom anvil temperatures are recorded to 0.1 °C by resistance temperature detectors and a microphone measures a sound signal which indicates the time at which an explosion occurs. The sample is heated by the anvils until it violently reacts.

MATERIALS

The PBXN-9 used is 92wt% HMX, 6 wt% dioctyl adipate (DOA) and 2 wt% carbonyl-terminated polybutadiene (HYTEMP 4454). Specifications for PBNX9 indicate that 55 wt% conform to Class I HMX particle size distribution and 45% conform to Class II particle size distribution. Pellets of PBXN-9 were uniaxially pressed in a mechanical pressing die at 138 MPa (20,000 psi) and ambient temperature to within 98% theoretical maximum density. The LLNL lot identification number is C-576 manufactured by American Ordnance (BAE 06F085-064).

CALCULATIONS

Reactions taking place during the final explosion are, in situations that do not involve shock stimuli, deflagrative in nature. Therefore, measurement of deflagration rate at high pressures and temperatures provides necessary information on runaway reaction behavior. This information is summarized in the burn rate equation,

$$B = aP^n \tag{1}$$

where B is the burn rate (mm/s), a is the burn rate coefficient (mm/s·MPa^n), P is the pressure (MPa) and n is the pressure exponent (dimensionless).

Additionally, an equation which follows a well known vivacity concept in combustion aids in quantifying the change in sample surface area available for deflagration and provides insight into overall explosion violence. This equation,

$$\frac{S}{S_o} = \left(\frac{1}{P^n} \frac{dP}{dt} \right) \frac{L}{a(P_f - P_o)} \tag{2}$$

is used to help characterize deflagration as either laminar or as “flame-spread” by calculating the deflagrating surface area, S, and normalizing it to the laminar deflagrating surface area, S_o, which is also the cross sectional area of the strand.[6] Written this way, laminar deflagration ($S/S_o \approx 1$) and flame-spread deflagration ($S/S_o >> 1$) regimes are more easily observed.

In Equation 2, the variable, P, is the time dependent chamber pressure (MPa), the constant, L, is the length (mm) of the deflagrating strand at t = 0, and the constants a and n are the burn rate parameters obtained from Equation 1. P_f and P_o are final and initial chamber pressure (MPa), respectively.

The LLNL hydrodynamics code Arbitrary Lagrangian-Eulerian in Three Dimensions (ALE3D) is used in many LLNL applications to predict both the timing and violence of thermal ignition events.[7-10] ALE3D includes the calculation of chemical reactions, thermal transport, and material movement and deformation. Most previous applications of ALE3D have used chemical reactions that exhibit Arrhenius temperature dependence and that depend on the concentration of one or more materials to the nth power, where n is an integer. Here, we assume that HMX decomposes independently of the binder and plasticizer in PBXN-9, where PBXN-9 consists of 92% HMX, 6% plasticizer, and 2% binder by mass. Recently, work has been done to refine an existing HMX kinetics model by Tarver and Tran[11] to provide improved agreement with Differential Scanning Calorimetry, Thermogravimetric Analysis, and One Dimensional Time-to-Explosion (ODTX) experiments.[12] Here, we apply this refined HMX kinetic model to the PBXN-9 chemical mixture. Tables 1 and 2 below provide values of kinetic parameters, reference densities, and energies of formation for the constituents of PBXN-9. The density, heat capacity and

thermal conductivity values for the HMX constituents were taken from previous studies,[11] the binder heat capacity and thermal conductivity were approximated as those for Viton A, and the properties for the plasticizer were approximated as those for engine oil.[13] Densities of the binder and plasticizer are known for PBXN-9 and are shown in Table 2. The energies of formation of the HMX gas components was determined by applying the LLNL Thermochemical code Cheetah[14] to create an LEOS database. Additional details regarding the material models are published elsewhere.[12]

Table 1. The updated HMX decomposition kinetics model[12]

Reaction*	**Kinetic Rate Expression**	**Parameter Values***
$\beta \leftrightarrow \delta$	$k = Ax_\beta \exp\left(-\frac{E}{RT}\right)\sinh\left(\Lambda^* - \frac{E_e^*}{RT}\right)$	E = 101.8 kcal/mol ln$A$/s^{-1} = 107.4 E_e^* = 2.32 kcal/mol Λ^* = 2.728
$\beta + \delta \leftrightarrow 2\delta$	$k = Ax_\beta x_\delta \exp\left(-\frac{E}{RT}\right)\sinh\left(\Lambda^* - \frac{E_e^*}{RT}\right)$	E = 27.0 kcal/mol ln$A$/s^{-1} = 29.5 E_e^* = 2.32 kcal/mol Λ^* = 2.728
$\beta \rightarrow f$	$k = Ax_\beta \exp\left(-\frac{E}{RT}\right)$	E = 52.7 kcal/mol ln$A$/s^{-1} = 50.05
$\delta \rightarrow f$	$k = Ax_\delta \exp\left(-\frac{E}{RT}\right)$	E = 52.7 kcal/mol ln$A$/s^{-1} = 50.11
$f \rightarrow hg$	$k = Ax_f \exp\left(-\frac{E}{RT}\right)$	E = 44.3 kcal/mol ln$A$/s^{-1} = 35.07
$f + hg \rightarrow 2hg$	$k = Ax_f x_{hg} \exp\left(-\frac{E}{RT}\right)$	E = 44.3 kcal/mol ln$A$/s^{-1} = 38.89
$hg + hg \rightarrow 2lg$	$k = Ax_{hg}^2 \exp\left(-\frac{E}{RT}\right)$	E = 34.1 kcal/mol ln$A$/s^{-1} = 27.57

*Symbols defined in the reactions are as follows:

β: β-HMX
δ: δ-HMX
f: HMX solid fragments
hg: HMX heavy gases
lg: HMX final products

Table 2. Density and Energy of Formation of PBXN-9 Mixture Components.

Mixture Component	Reference Density (g/cm^3)	Energy of Formation (cal/g)
β-HMX	1.865	0.0
δ-HMX	1.755	+10.0
HMX solid fragments	1.755	+70.0
HMX heavy gases	1.865	from LEOS database
HMX final products	1.865	from LEOS database
Binder	1.100	0.0
Plasticizer	0.927	0.0

RESULTS AND DISCUSSION

DEFLAGRATION RATE MEASUREMENTS

The pressure dependent deflagration rate of PBXN was measured between 0 and 310 MPa in a series of 5 burn tower experiments. Prepresserization of the towers varied in order to achieve a wide pressure range for the set yet still have overlapping pressures points from one tower to the next. Results of these experiments are plotted in Figure 6 along with the pressure dependent deflagration rate of LX-04 (see Table 3 for constituents).

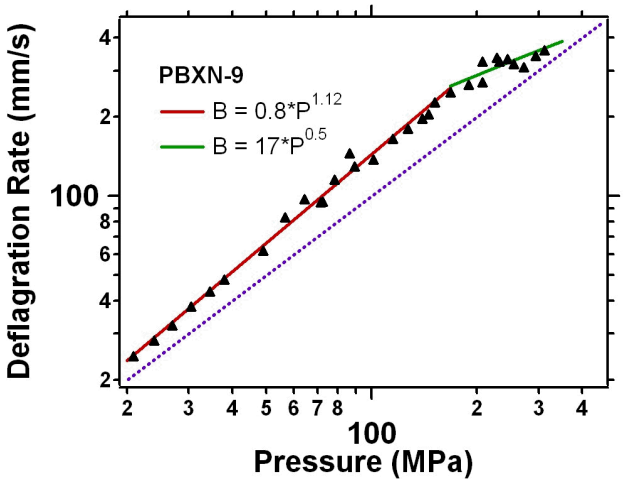

Figure 6. PBXN-9 pressure dependent deflagration rates

Changes in the material's deflagration behavior at various pressures necessitated a change in the burn fit variables. The data were split into two parts; the low pressure range was 0-168 MPa, the high pressure range was 168-310 MPa. The decision to split the data at 168 MPa was based on a chi-squared minimization of the combined high and low pressure regions. Using a Levenberg-Marquart chi-squared minimization method the log of the pressure vs. the log of the burn rate was fit to a line for each pressure regime. The slope and intercept were used to determine the burn rate coefficient and pressure exponent in equation 1. The burn rate coefficients and pressure exponents are listed in Figure 6. PBXN-9 shows a decreasing pressure exponent at elevated pressures indicating a decreased sensitivity or slowing of the burn rate at higher pressures.

Surface area calculations were performed using equation 2 and the burn rate coefficients and pressures exponents. Figure 7 displays the normalized surface area and vivacity for a single tower. In this example, the initially sharp rise in surface area and vivacity at t = 0 correspond to the ignition of the $BKNO_3$/NHS pellet. Figure 8 shows the normalized surface are and vivacity for all the towers. Based on

these surface area calculations and the deflagration rate data it is evident that, in the pressure regime studied, PBXN-9 burns in a laminar manner.

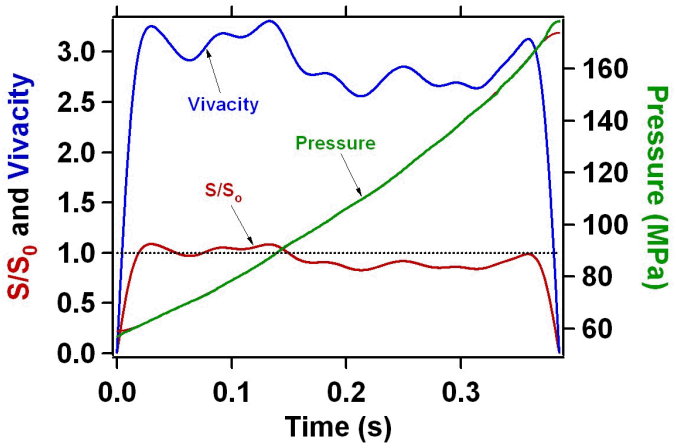

Figure 7. PBXN-9 single tower surface area and vivacity

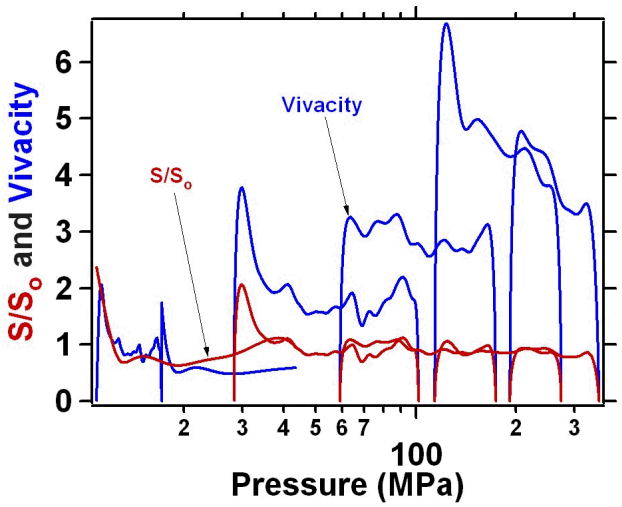

Figure 8. PBXN-9 surface area and vivacity

Unlike PBXN-9 many other HMX based materials do not burn in a laminar manner over the same pressure range. Figure 9 shows the deflagration rate vs. pressure for LX-07 which was measured in a previous study.[3] At low pressures, the deflagration is similar to that of LX-04, however, above ca. 200 MPa, the deflagration becomes rapid and erratic, indicative of a convective or non-laminar burning that results from deconsolidation of the material.[3] Studies of LX-10 and PBX-9501 also demonstrate convective burning at pressures above 150 MPa.[3] Generally, convective burning results in more violent explosions as has been demonstrated by scaled thermal explosion experiments at LLNL.[15]

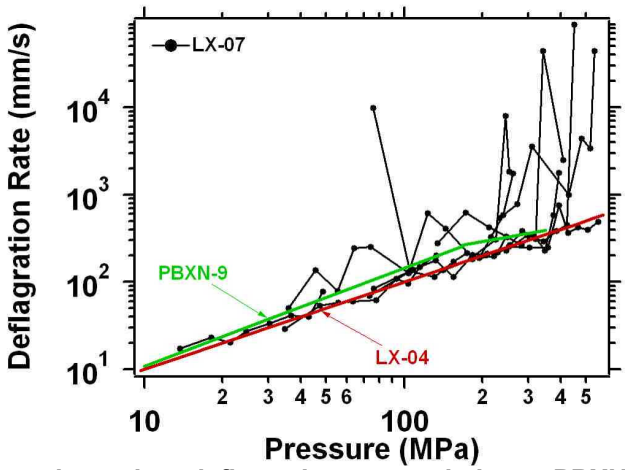

Figure 9. LX-07 pressure dependent deflagration rates relative to PBXN-9 and LX-04 (reproduced with permission from REF [3])

Based on these LX-07 and LX-10 studies it was previously hypothesized that the higher weight percent of HMX may produce convective burning.[3] Studies of PBX-9501 indicate that the reactivity of the binder also plays a role in the burn characteristics. Our PBXN-9 results appear indicate that the amount of HMX is not the only factor as PBXN-9 contains a similar amount of HMX as LX-07, LX-10, and PBX-9501 (see Table 3). This difference could be due to the nature of the binder/plasticizer in PBXN-9 or the thickness of the binder/plasticizer coating on the HMX grains.

Due to the low density of the binder/plasticizer in PBXN-9 there is significantly more binder/plasticizer then that found in the high-density Viton A based explosives. Table 3 lists the calculated percent volume in each material; a comparison of the relative volumes indicates that PBXN-9 is more akin to LX-04. The HMX grain coating thickness was calculated[16] using equation 3:

$$T = \Phi_p d_e \rho_e / 6\rho_p \quad (3)$$

Where T is the coating thickness, Φ_p is the weight fraction of binder/plasticizer, d_e is the mean HMX particle diameter and ρ with the subscript 'e' and 'p' are the densities of the explosive and binder/plasticizer respectively. The mean particle diameter was estimated by taking the weighted average of each sieve size group; for example, all the particles that pass through the 44 μm sieve were assumed to have a diameter of 44 μm. This method uniformly overestimates the particle diameters for all the materials. For PBXN-9 and PBX-9501 the density of the binder/plasticizer was a weighted average of the constituent binder and plasticizer.

Table 3 lists the mean particle diameter and calculated coating thickness. PBXN-9 has the thickest coating, yet it is clear that the deflagration behavior of all of these materials is not simply due to the thickness of the coating. Instead, the difference between PBXN-9 and the three non-laminar burning materials may be due to the mechanical or thermal properties of the binder/plasticizer alone or in conjunction with the amount of binder/plasticizer. Generally, the binder/plasticizer in PBXN-9 is more malleable than Viton A or the binder/plasticizer in PXN-9501. The stiffer materials crack under pressure whereas PBXN-9 may deform without cracking.

Table 3: HMX based formulations details and deflagration summary

Material	Deflagration Behavior	Particle Diameter[a] (μm)	Coating Thickness (μm)	Constituents	Density (g/cm^3)	Wt %	Vol %
LX-04	Laminar Burn[b]	68	1.78	HMX	1.91	85	84.6
				Viton A	1.85	15	15.4
LX-07	Convective burn above 200 MPa[b]	68	1.19	HMX	1.91	90	89.7
				Viton A	1.85	10	10.3
LX-10	Convective burn above 150 MPa[b]	171	1.64	HMX	1.91	94.5	94.3
				Viton A	1.85	5.5	5.7
PBX-9501	Convective burn above 150 MPa[b]	171	2.12	HMX	1.91	95	92.7
				Estane	1.18	2.5	3.9
				BPNPA/F	1.385	2.5	3.3
PBXN-9	Laminar Burn	144	3.78	HMX	1.91	92.8	86.8
				DOA	0.927	5.3	10.2
				HYTEMP 4454	1.1	1.9	3.1

[a]Mean particle diameter calculated using sieve size and population that passes through. This is an overestimate of the particle size for all materials. [b]See ref [3] for deflagration results.

TIME TO EXPLOSION MEASUREMENTS

ODTX measurements of PBXN-9 are shown relative to other HMX based explosives in Figure 10. Careful examination of the Figure 10 reveals small differences between PBXN-9 and the other HMX based materials. Variability from one material to the next is still under investigation and may be due to the thermal properties of the binder/plasticizers in each material (e.g. thermal conductivity, heat capacity, melting points). Generally these materials all appear to explode on similar timescales at the same temperature indicating that the dominant factor in these experiments is the type of explosive.

ODTX simulations were carried out using a 160-element, axisymmetric two-dimensional piton mesh as shown in Figure 11, which represents a 5º cone from the center of the 0.5-inch ODTX sphere to the isothermal surface. An explosion was deemed to occur when one of three criteria was met: the temperature rise anywhere in the explosive exceeded 10^9 K/s, the temperature anywhere in the explosive exceeded 1000K, or the mass fraction of HMX final products exceeded 5% anywhere in the explosive. Figure 12 shows that the calculated explosion times are in agreement with experiment with an average error of 123%, which is larger than the 30% error calibrated for LX-10 previously[12] and is most likely due to uncertainty in the material properties of the binder and plasticizer and any effects due to decomposition of the binder and plasticizer. Nevertheless, Figure 12 shows a calculated ODTX curve slope that is consistent with the experimental data. This figure also shows that doubling the mesh resolution results in negligible changes in predicted explosion times except at the highest temperatures, where the maximum change in calculated explosion time is 7%.

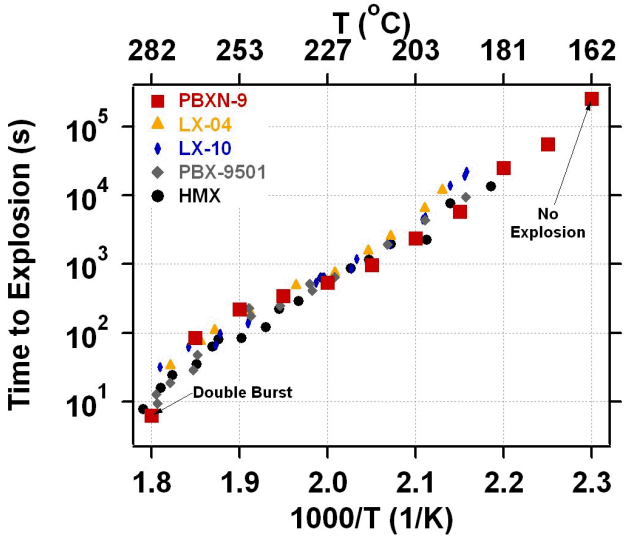

Figure 10. PBXN-9 times to explosion (red squares) relative to HMX and HMX-binder explosives

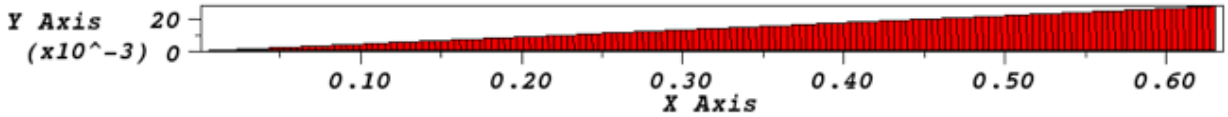

Figure 11. Mesh used in ODTX simulations. Axisymmetry is applied along the x-axis, and dimensions are in cm.

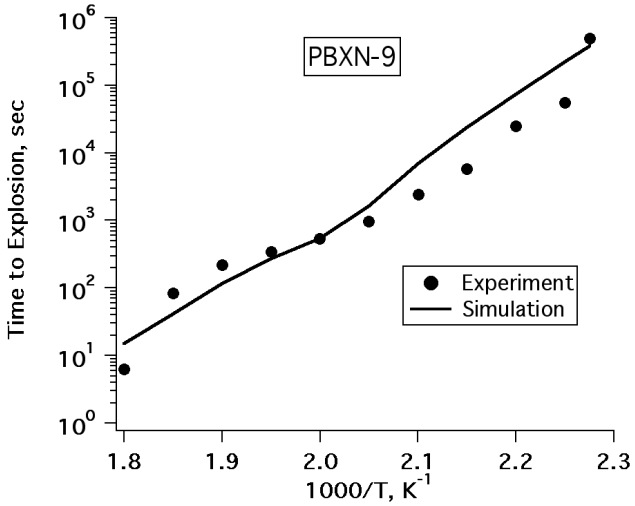

Figure 12. Comparison of experimental and simulated ODTX explosion times.

SUMMARY AND CONCLUSIONS

The ignition times and deflagration rates of PBXN-9 were studied and compared to similar HMX based materials including LX-04, LX-07, LX-10 and PBX-9501. Ignition times were measured using LLNL's one dimensional time to explosion (ODTX) apparatus and modeled using ALE3D. The experimental and modeling results indicate that the dominant factor controlling the ignition time is the type of explosive. Variability in the amount and type of non-explosive material (i.e. binder and/or plasticizer) plays a minor role in the ignition kinetics. Variability in the amount of HMX is expected to affect the

ignition kinetics, however, at this limited range (85-95 wt%) there appears to be little difference between the materials. Measurements of the violence of these ODTX experiments are underway and will provide further insight into nature of these HMX based materials.

Using the LLNL designed high pressure strand burner, the pressure dependent deflagration rate of PBXN-9 was investigated between 0 and 310 MPa. Results of these studies indicate that PBXN-9 burns in a laminar manner over the full pressure range and does not convectively burn suggesting that it does not deconsolidate. This burn behavior is different from that measured previously for LX-07, LX-10, and PBX-9501, all of which display convective burning at pressures greater than 150 MPa.[3] This observed difference in deflagration behavior is attributed to the material properties alone or in combination with the high volume of binder/plasticizer present. Ultimately, the presence of non-laminar burn correlates with the violence of the thermal explosion, and scaled thermal explosion experiments indicate that the cookoff of both PBXN-9 and LX-04 are less violent than LX-07, LX-10 and PBX-9501. Further work is underway and will explore the deflagration rate up to 450 MPa and the effect of thermally soaking the PBXN-9 prior to deflagration.

ACKNOWLEDGEMENTS

We gratefully acknowledge Franco Gagliardi and Gary Hust for their contributions to this experimental effort and Mark Hoffman for helpful discussion. This work performed under the auspices of the U.S. Department of Energy by Lawrence Livermore National Laboratory under Contract DE-AC52-07NA27344.

REFERENCES

[1] J. L. Maienschein and J. B. Chandler, "High Pressure Laminar Burn Rates of AP/AI/HTPB Propellants" *JANNAF 34th Combustion and 16 Propulsion Systems Hazards Subcommittee Meetings*, **1997**, II, 95.

[2] J. L. Maienschein, E. L. Lee, J. E. Reaugh, C. I. Merrill and R. R. Lambert, "Modeling the Impact Response of Booster Propellants" *JANNAF 34th Combustion and 16 Propulsion Systems Hazards Subcommittee Meetings*, **1997**, II, 163.

[3] J. L. Maienschein, J. F. Wardell, M. R. DeHaven and C. K. Black, "Deflagration of HMX-Based Explosives at High Temperatures and Pressures" *Propellants, Explosives, Pyrotechnics*, **2004**, 29, 287.

[4] A. Birk, D. E. Kooker and P. Baker, "Model of Cavity Combustion Within an Energetic Solid: Application to Composition-B" *JANNAF 37th Combustion and 19th Propulsion Systems Hazards Subcommittee Meetings*, **2000**, II, 95.

[5] R. Lieb and P. Baker, "Combustion Morphology of TNT and Composition B" *JANNAF 37th Combustion and 19th Propulsion Systems Hazards Subcommittee Meetings*, **2000**, II, 81.

[6] J. G. Koerner, J. L. Maienschein, C. K. Black and M. R. DeHaven, "Laminar and Deconsolidative Deflagration of RDX-based Explosives at High Pressures" *13th International Detonation Symposium*, **2006**, 527.

[7] J. J. Yoh, M. A. MacClelland, J. L. Maienschein, J. F. Wardell and C. M. Tarver, "Simulating thermal explosion of cyclotrimethylenetrinitroamine-based explosives: model comparisons with experiment" *J. Appl. Phys.*, **2005**, 97, 083504.

[8] A. K. Burnham, R. K. Weese, A. P. Wemhoff and J. L. Maienschein, "A Historical and Current Perspective on Predicting Thermal Cookoff Behavior" *Journal of Thermal Analysis*, **2007**, 89, 407.

[9] A. P. Wemhoff, A. K. Burnham and A. L. Nichols III, "Application of Global Kinetic Models of HMX b-d Transition and Cookoff Processes" *J. Phys. Chem. A*, **2007**, 111, 1575.

[10] A. P. Wemhoff, A. K. Burnham and J. L. Maienschein, "Global Kinetic Models of AP/AL-Based Propellants" *JANNAF 41st CS, 29th APS and 23rd PSHS Joint Meeting*, **2006**, 1.

[11] C. M. Tarver and T. D. Tran, "Thermal Decomposition Models for HMX-based Plastic Bonded Explosives" *Combustion and Flame*, **2004**, 137, 50.

[12] A. P. Wemhoff, M. H. Howard, A. K. Burnham and A. L. Nichols III, "An HMX Kinetic Model Calibrated Using Simulations of Multiple Small-scale Thermal Safety Tests" *J. Phys. Chem. A*, **2007**, Submitted.

[13] F. P. Incropera and D. P. DeWitt, *Fundamentals of Heat and Mass Transfer* 4th, Wiley: New York, NY, 1996.

[14] L. E. Fried, M. H. Howard and P. C. Souers, "Cheetah 3.0 User's Manual" **2000**, Report UCRL-MA-117541-REV-6.

[15] J. L. Maienschein, J. F. Wardell, R. K. Weese, B. J. Cuningham and T. D. Tran, "Understanding and Predicting the Thermal Explosion Violence of HMX-based and RDX-based Explosives- Experimental Measrurements of Material Perperties and Reaction Violence" *12 Int. Det. Symp.*, **2002**, 846.

[16] D. M. Hoffman, "Dynamic Mechanical Signatures of Viton A and Plastic Bonded Explosives Based on This Polymer" *Polymer Eng. and Sci.*, **2003**, 43, 139.